Nanostructured Ferrite as Photocatalysts for H_2 Generation from Water Splitting and Sunlight

Mercedes Yudith Ortega-López, Jesús Manuel Salinas-Gutiérrez, Alejandro López-Ortiz, Virginia Collins-Martínez*

Centro de Investigación en Materiales Avanzados S. C., Laboratorio Nacional de Nanotecnología, Depto. de Materiales Nanoestructurados, Miguel de Cervantes 120, C. P. 31109, Chihuahua, Chih. México.
*Tel: +52 614 436 1129, Fax: +52 614 439 1130: e-mail: virginia.collins@cimav.edu.mx

ABSTRACT

Materials with higher efficiency and activated under the sunlight spectrum (band gap energy from 1.5 to 3.0eV) are today´s trends in newer photocatalysts for the hydrogen generation. The aim of the present study is to investigate alternative semiconductor materials to titanium dioxide for the generation of hydrogen with band gap energy values lower than that of TiO_2 (<3.2eV). Examples of these are some transition metal ferrites such as $CuFe_2O_4$, $CoFe_2O_4$ and $NiFe_2O_4$. These ferrites were prepared by co-precipitation and heat treatment. Characterization was performed by XRD, BET, SEM, TEM and UV-Vis spectroscopy. Photocatalytic activity evaluation of the materials for hydrogen generation from water splitting under visible light was followed by gas chromatography. Results indicate that these materials showed corresponding spinel crystalline phases and nanometer particle sizes. Photocatalytic evaluation of these ferrites under visible light showed H_2 yields up to 10.8 mmoles/g_{cat}. These yields compared with those reported in the literature indicate that these materials can be considered as promising photocatalysts for hydrogen generation.

Keywords: Ferrites, Nanoparticles, Photocatalytic activity, Water splitting

1. INTRODUCTION

The adverse environmental impact and the near depletion of fossil fuels, which are currently the preferred energy sources, represent the main motivations in seeking alternative energy sources from renewables. In this context, solar energy as an infinite resource [1] and the production of hydrogen as an energy carrier [2], are a clear option to clean, economical and sustainable energy generation through the use of fuel cells. In this context the hydrogen production from solar energy [3] and through the process of photocatalytic water-splitting represents a feasible clean energy alternative.

Within hydrogen production from photocatalytic water-splitting it is important to consider three main factors [3]: first, solar energy must be efficiently absorbed to generate pairs of electrons and holes for the dissociation of water, second, H_2 and O_2 recombination must proceed in order to reform the water molecule again and third, possible undesirable reactions may take place (corrosive reactions).

For the photocatalytic process to occur some conditions are needed to obtain a viable process. Since 1972, when Fujishima and Honda once successfully used by the first time TiO_2 photo-anodes in the evolution of hydrogen, while the use of semiconductor oxides has been considered a promising path for a sustainable hydrogen production [4]. From this fundamental study, an important amount of research has focused in finding alternate semiconductors to TiO_2 Degussa P25 (material usually used as a reference photocatalyst) with equal or better activity towards the hydrogen production under the UV or visible light irradiation. One of the main disadvantages that TiO_2 presents is that the energy needed for its activation is found under the UV light spectrum (~3.2 eV). Therefore, it is a reasonable strategy to explore other materials capable to be activated under the visible light spectrum and that present equal or better efficiencies towards the hydrogen production through the water splitting process.

One example of such materials is the ferrites, which have been considered as a novel option in photocatalytic processes.

Dentro de este grupo de materiales las ferritas han sido estudiadas como una opción novedosa como fotocalizador. Entre sus principales características se encuentran sus excelentes propiedades magnéticas, alta conductividad electrónica, alta estabilidad térmica, su efectiva actividad catalítica [5] , su resistencia a la corrosión [3] y sobre todo un ancho de banda prohibida que se encuentra dentro del espectro de luz visible (1.4 eV) [1]. Among their main features are their excellent magnetic properties, high electronic conductivity, high thermal stability, their effective catalytic activity [5], its corrosion resistance [3] and mostly a forbidden band gap energy within the range of visible light (1.4 eV) [1]. Therefore, the objective of the present research is aimed on the synthesis, characterization and

photocatalytic evaluation of ferrite nanoparticles towards the hydrogen production using methanol as sacrificial reagent under visible light irradiation.

2. EXPERIMENTAL

2.1. Synthesis

$CuFe_2O_4$, $CoFe_2O_4$ and $NiFe_2O_4$ were prepared by the method of chemical co-precipitation using the corresponding metal nitrate solutions and NaOH as a precipitating agent followed by a thermal treatment (see Figure 1). Stoichiometric amounts of nano-hydrated ferric nitrate, 2.5 hydrated copper nitrate and hexa-hydrated cobalt and nickel nitrates were used to prepare the corresponding nitrate solutions [6]. Using a peristaltic pump, these nitrates were slowly added at a rate of 5 ml/min to the precipitating agent solution (NaOH). The reacting mixture was kept under constant stirring and a basic pH of 13 using NaOH under constant stirring. This basic pH was required to influence the precipitation reaction rate of the complex, since a highly alkaline medium generates smaller (precipitate) size particles [6]. In order to obtain a nanoparticulate crystalline material the resulting solution was dried and exposed to a low temperature thermal treatment at 250°C for 6 hours, followed by 1 hour at 350°C. This precipitate was the allowed to cool to room temperature. Finally, the product was washed with distilled water and ethyl alcohol to eliminate any residue, then filtered and dried at 80°C by 4 hours to follow its characterization and photocatalytic evaluation.

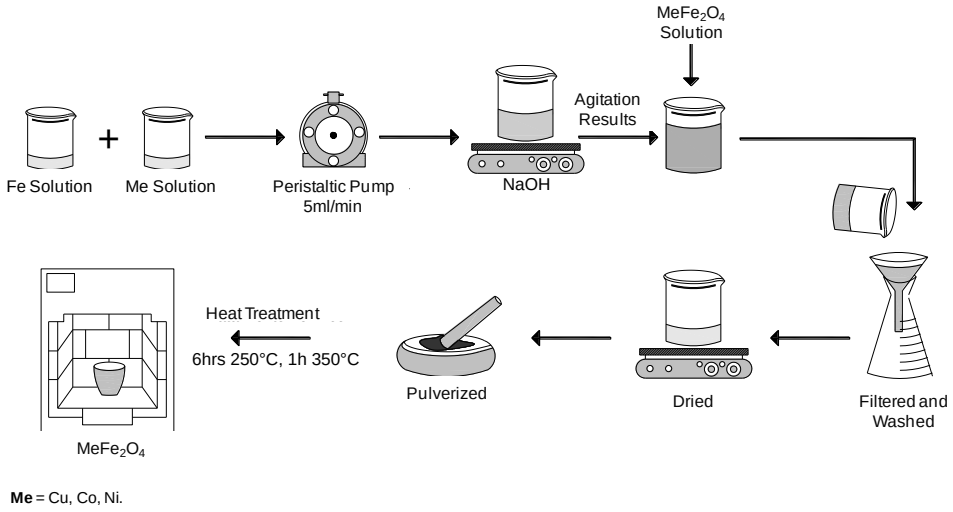

Figure 1. Procedure for the synthesis of $CuFe_2O_4$, $CoFe_2O_4$ and $NiFe_2O_4$ nanoparticles through co-precipitation.

2.2. Powder Characterization

Samples crystalline phase was determined by X-ray diffraction (XRD) using a PANalytical diffractometer model X'Pert PRO equipped with a X'Celerator detector. From the X-ray diffraction patterns information and through the use of the Scherrer equation, the crystal size of the materials was calculated. The specific surface area of the materials was estimated by N_2 physisorption using the BET technique on an Autosorb-1, Gas Sorption System (Quantachrome Corporation). The homogeneity in chemical composition of the samples was determined through dispersive X-ray spectroscopy (EDS) mapping using a detector coupled to a scanning electron microscope model 5800-LV Jeol JSM brand. The particle size of the materials and their morphology was determined by transmission electron microscopy (TEM) using a Philips CM-200. The light absorption spectrum of the materials was obtained through UV-visible spectroscopy (UV/Vis) by a Perkin Elmer spectrophotometer model Lambda 10 equipped with integrating sphere.

2.3. Photocatalytic Evaluation

Figure 2 shows a scheme of the experimental system employed for the photocatalytic evaluation of the materials, which consists of a photoreactor, artificial lighting and data collection analysis equipment. The photoreactor was built using a quartz tube with a 5 and 19 cm diameter and length, respectively where a suspension of each nanoparticle material ($CuFe_2O_4$, $CoFe_2O_4$ y $NiFe_2O_4$) was placed. Two aluminum flanges bolted together by threaded rods were used to close the tube and its sealing was achieved through neoprene o-rings. The radiation source used was a white light artificial mercurial lamp of 120 W, GE. Concentration of initial reagents and changes in gas phase composition within the photoreactor during the course of the experiments was determined by gas chromatography (GC) using a Clarus 500, Perkin Elmer, equipped with thermal conductivity (TCD) and flame ionization (FID) detectors arranged in series. The sampling of the gas was performed through a septum sampling port located on one side of the photoreactor and transferred to the GC by hand injection using a 1 ml special syringe for gases.

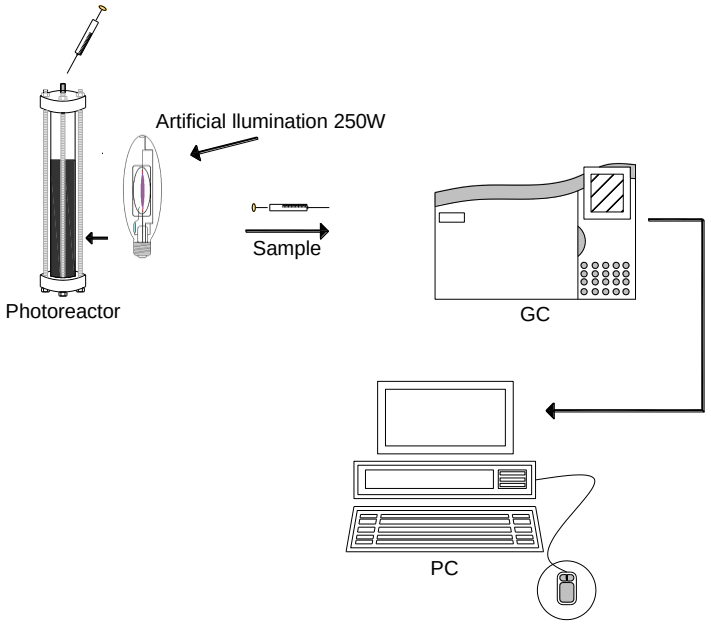

Figure 2. Experimental setup system for the photocatalytic evaluation of the nanomaterials.

The photoreactor was hermetically sealed and checked for leaks. The photocatalytic suspension consisted of a mixture of distilled water and ethanol as a sacrificial reagent (50:1 molar ratio) and 200 mg of photocatalyst, which was artificially, irradiated using a visible light lamp. Prior to the photocatalytic evaluation the reactor was covered to prevent it from light exposure and was subjected to constant stirring for 15 minutes in order to achieve good homogenization of the suspension in the photoreactor. The initial concentration of gases was evaluated by gas sampling of the gas phase within the photoreactor and analyzed by GC. Then the mercury lamp was turned on and a gap of seven inches was left between the lamp and the photoreactor reactor wall. Sampling was performed manually every hour to complete twenty two hours of irradiation. Analysis of the initial gas phase concentration and of changes in gas composition inside the reactor was performed by means of gas chromatography (GC, Perkin Elmer Clarus 500), compounds separation used a Carboxen 100 packed column coupled with a thermal conductivity detector (TCD). Product identification was achieved by determining the elution time with respect to pure reagent concentrations and the quantification was performed using calibration curves.

3. RESULTS AND DICUSSION

3.1. X-ray Diffraction (XRD)

Figure 3 presents results of XRD characterization for samples $CuFe_2O_4$, $CoFe_2O_4$ and $NiFe_2O_4$

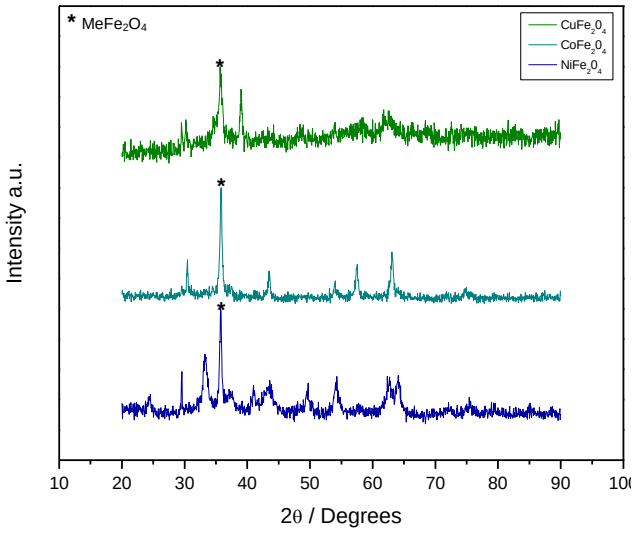

Figure 3. XRD patterns of the ferrites studied in the present research study.

For the copper ferrite sample CuO and $CuFe_2O_4$ phases were found in the XRD diffractogram, while for the case of the cobalt ferrite sample only the $CoFe_2O_4$ phase was present and in the particular case of sample nickel ferrite two phases were found; Fe_2O_3 and $NiFe_2O_4$. Haihua, et al 2009 [3] reported a diffraction pattern with the same phases as those for sample $CuFe_2O_4$. Whereas, the cobalt ferrite diffraction pattern is consistent with the one reported by Hua, et al, 2008 [7].

3.2. Scanning Electron Microscopy (SEM)

Figure 4 shows SEM images of samples $CuFe_2O_4$, $CoFe_2O_4$ and $NiFe_2O_4$. In this Figure it can be observed that in all cases it can be observed agglomerated particles with irregular morphologies (spherical, flake-like or needle), which are in the order of nanometers. Here it can be concluded that a careful control of the nitrate addition during the precipitation process has a significant effect in obtaining nano-sized particles as can be seen in the SEM images [6].

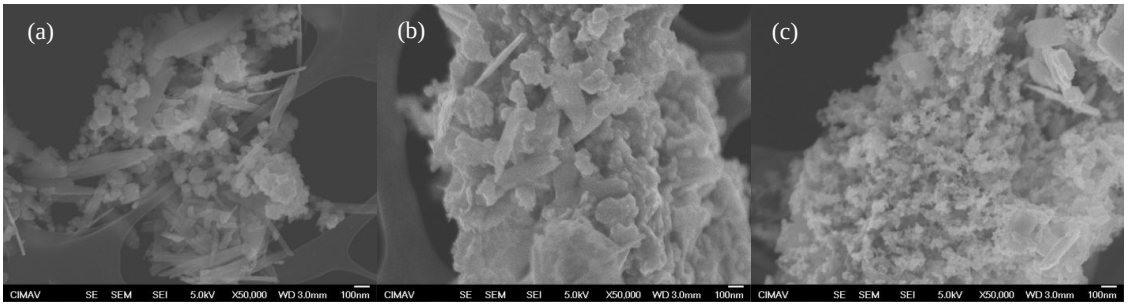

Figure 4. SEM Images of (a) $CuFe_2O_4$, (b) $CoFe_2O_4$ and (c) $NiFe_2O_4$.

3.3. Transmission Electron Microscopy (TEM)

Morphology for the case of sample $CuFe_2O_4$ (see Figure 5a) is composed by agglomerate particles of irregular shapes with sizes varying between 15 and 30 nm, the same morphology was reported by Haihua, et al 2009 [3] for copper ferrites. While, for cobalt (b) and nickel (c) ferrites it can be observed sizes of around 25 nm. Here also, very similar particle sizes were reported by Hua et al, 2008 [7] for both kind of samples.

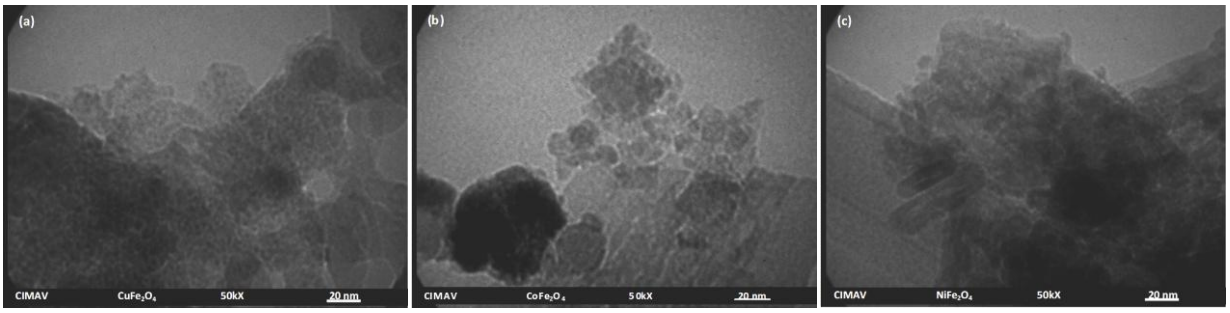

Figure 5. TEM images at 50kX for samples (a) $CuFe_2O_4$, (b) $CoFe_2O_4$ and (c) $NiFe_2O_4$.

3.4. BET Surface Area

It is well known that surface area is directly influenced by the particle size and at the same time closely related to the method of synthesis being employed. The specific surface areas of the photocatalysts were 32, 21 and 24 m^2/g for samples $CuFe_2O_4$, $CoFe_2O_4$ and $NiFe_2O_4$, respectively.

Figure 6 shows the BET adsorption isotherms obtained for the synthesized samples in the present research. The above reported values of surface area can be explained in terms of the shapes of these isotherms. For the case of

sample $CuFe_2O_4$ the presence of hysteresis and a type IV is an indication of a porous material, while samples $CoFe_2O_4$ and $NiFe_2O_4$ present type III isotherms with negligible hysteresis and consequently porosity.

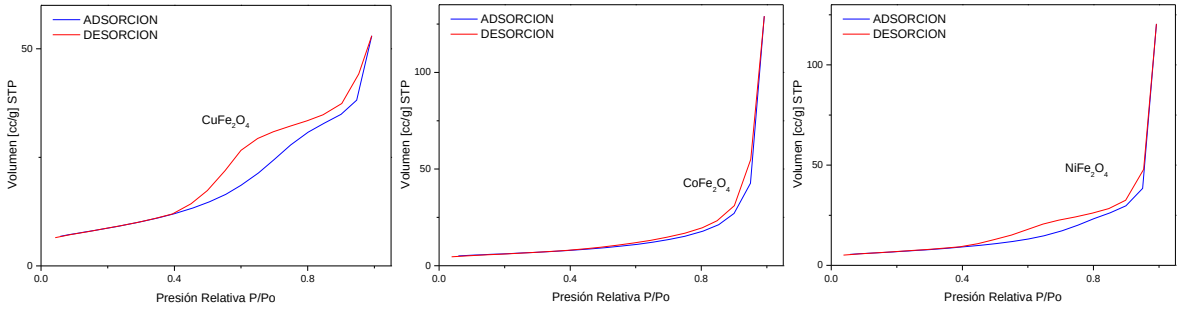

Figure 6. BET adsorption Isotherms for samples (a) $CuFe_2O_4$, (b) $CoFe_2O_4$ and (c) $NiFe_2O_4$.

3.5. UV/Vis Spectroscopy

UV/Vis diffuse reflectance spectra for samples of $CuFe_2O4$, $NiFe_2O_4$ $CoFe_2O_4$ and are presented in Figure 7. Here, the edge energy of the forbidden band can be calculated from the reflectance data by the Kubelka-Munk function.

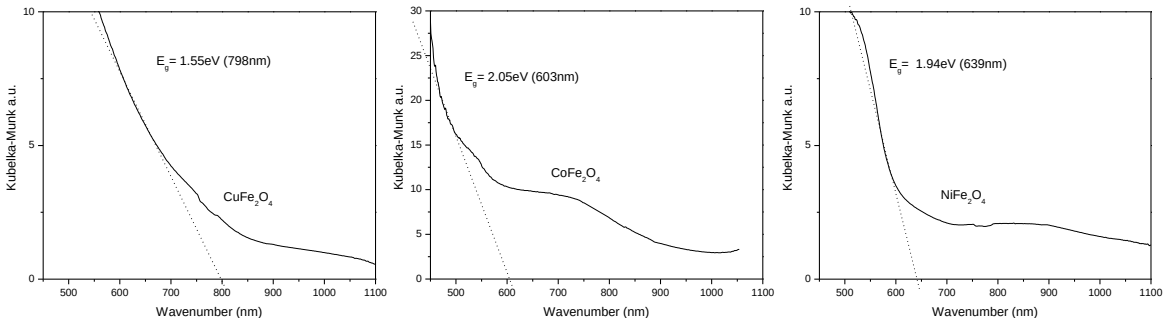

Figure 7. UV/Vis diffuse reflectance spectra from samples (a) $CuFe_2O_4$, (b) $CoFe_2O_4$ and (c) $NiFe_2O_4$.

From this Figure it can be observed that UV/Vis spectra for all samples fall within the visible light range. The band gap energy value for samples $CuFe_2O_4$, $CoFe_2O_4$ and $NiFe_2O_4$ were 1.55, 2.05 and 1.94 eV, respectively. Therefore, it can be concluded that these materials presumably work as photocatalysts within the visible light spectrum. These values are consistent with the ones reported in the literature. For example, a value of 1.42 eV is reported for $CuFe_2O_4$ by Kezzim, et al 2011 [1], a band gap of ~ 1.5 eV for $CoFe_2O_4$ reported by Limei, et al 2011 [8], while a value of 2.19 eV for $NiFe_2O_4$ is reported by Erik, et al 2012 [9].

3.6. Photocatalytic Activity

Photocatalytic evaluation of the synthesized materials was carried out by follow up of the hydrogen production by gas chromatography.

Figure 8 show results from the photocatalytic evaluation of the synthesized materials. In this Figure, the hydrogen evolution in micro-mols per gram of catalyst ($\mu m/g_{cat}$) as a function of time is plotted for each tested photocatalyst. Here it can be seen that the superior performance of the ferrites with respect to TiO_2 (P25) is evident.

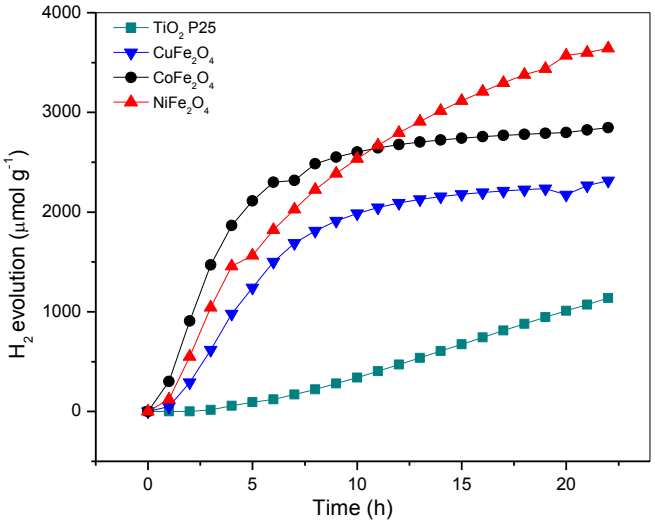

Figure 8. Hydrogen evolution profile for the synthesized materials as a function of time.

Otherwise, Table 1 show values of hydrogen evolution in micro-mols per gram of catalyst ($\mu m/g_{cat}$) after a total of 22 hours of reaction taken from results presented in Figure 8 and these are compared to TiO_2 (P25). The order from higher to lower hydrogen production was: $NiFe_2O_4$ > $CoFe_2O_4$ > $CuFe_2O_4$, which values were well above the obtained, for reference TiO_2 (P25). This behavior can be attributed to the fact that the ferrites are materials whose characteristics meet the conditions for carrying out the electron-hole pair reaction needed for good photocatalytic activity [9,10].

Table I. Hydrogen generation (%) as a function of time after 22 hours of irradiation

Material	H_2 Evolution @ 22 h ($\mu m/g_{cat}$)
TiO_2 (P25)	1138
$CuFe_2O_4$	2315
$CoFe_2O_4$	2846
$NiFe_2O_4$	3643

4. CONCLUSIONS

$CuFe_2O_4$, $NiFe_2O_4$ and $CoFe_2O_4$ nanoparticles were synthesized by a chemical co-precipitation method followed by heat treatment and tested for hydrogen production, demonstrating that the present synthesis technique is a simple, inexpensive and reproducible. For samples of $NiFe_2O_4$ and $CuFe_2O_4$ the dominant crystal structure is that of a spinel $MeFe_2O_4$ (Me = Cu, Ni) accompanied with formation of Fe_2O_3 and CuO, respectively. For the case of the $CoFe_2O_4$ sample the crystallographic structure of spinel $CoFe_2O_4$ is the only crystallographic phase present in the sample. SEM results indicate that in all cases nanoparticles were obtained with a wide variety of nanoscale morphologies ranging from spherical to flakes or needles. Photocatalytic evaluation towards hydrogen production resulted in a superior behavior of nickel, cobalt and copper ferrites compared to results obtained for reference TiO_2 (P25) photocatalyst. The order from higher to lower hydrogen production was: $NiFe_2O_4$ > $CoFe_2O_4$ > $CuFe_2O_4$. The good photocatalytic activity of the synthesized samples is related to the inherent properties of these materials, demonstrating that meet necessary conditions to carry out the electron-hole pair reaction required for good photocatalytic activity.

ACKNOWLEDGEMENTS

The authors are grateful to M Sc. Enrique Torres, M Sc. Karla Campos, Eng. Wilber Antunez, M Sc. Raul Ochoa and Eng. Luis de la Torre for their help on XRD, SEM, TEM, BET and UV-Vis spectroscopy characterization, respectively. Also to CIMAV, S. C and CONACYT for their financial assistance.

REFERENCES

[1]A. Kezzim, N. Nasrallah, A. Abdi, M. Tari,Visible light induced hydrogen on the novel hetero-system $CuFe_2O_4/TiO_2$; Energy Conversion and Management 52 (2011) 2800–2806. 2800–2806.

[2]N. Shimoda , K. Faungnawakij, R. Kikuchi, T. Fukunaga, K. Eguchi, Catalytic performance enhancement by heat treatment of $CuFe_2O_4$ spinel and g-alumina composite catalysts for steam reforming of dimethyl ether; Applied Catalysis A: General 365 (2009) 71–78.

[3]Haihua Yang, Jianhui Yan, Zhouguang Lu, Xiang Cheng, Yougen Tang, Photocatalytic activity evaluation of tetragonal $CuFe_2O_4$ nanoparticles for the H_2 evolution under visible light irradiation; Journal of Alloys and Compounds 476 (2009) 715–719.

[4]Zhonghai Zhang, Md. Faruk Hossain, Takakazu Takahashi, Photoelectrochemical water splitting on highly smooth and ordered TiO_2 nanotube arrays for hydrogen generation; International Journal of Hydrogen Energy 35, 16 (2010) 8528–8535.

[5]N.M. Deraz, Production and characterization of pure and doped copper ferrite nanoparticles/Pyrolysis; J. Anal. Appl. 82 (2008) 212–222.

[6]M.Y. Ortega-López, J.M. Salinas-Gutiérrez, V. Guzmán-Velderrain, A López-Ortiz, V. Collins-Martínez, Alternate Semiconductor Materials to TiO_2 as Photocatalysts for the Degradation of Organic Compounds (2012).

[7]Chaoquan Hua, Zhenghong Gaoa, Xiaorui Yangb, One-pot low temperature synthesis of MFe_2O_4 (M ¼ Co, Ni, Zn) superparamagnetic nanocrystals; Journal of Magnetism and Magnetic Materials 320 (2008) L70–L73.

[8]Xue Limei, Zhang Fenghua, Chen Bin, Bai Xuefeng, Preparation of Light-Driven Spinel Nanoparticles $CoAl_2O_4$, $MgFe_2O_4$ and $CoFe_2O_4$ and Their Photocatalytic Reduction of Carbon Dioxide; ISBN: 978-0-7695-4350-5 (2011).

[9]Erik Casbeer, Virender K. Sharma, Xiang-Zhong Li, Review: Synthesis and photocatalytic activity of ferrites under visible light: A review; Separation and Purification Technology 87 (2012) 1–14.

[10]Hong Deng, Hongyu Chen, He Li, Synthesis of crystal MFe_2O_4 (M = Mg, Cu, Ni) microspheres; Materials Chemistry and Physics 101 (2007) 509–513.